energies

MDPI

Article

High-Power Induction Motors Supplied with Voltage Containing Subharmonics

Piotr Gnaciński [1,*] and Piotr Klimczak [2]

[1] Department of Ship Electrical Power Engineering, Faculty of Marine Electrical Engineering, Gdynia Maritime University, 81-225 Gdynia, Poland
[2] Diagnostic and Service of Electrical Motors Department, Zakład Maszyn Elektrycznych "EMIT" Cantoni Group, 99-320 Żychlin, Poland; piotr.klimczak@cantonigroup.com
* Correspondence: p.gnacinski@we.umg.edu.pl; Tel.: +48-58-5586-382

Received: 14 October 2020; Accepted: 10 November 2020; Published: 12 November 2020



Abstract: In some power networks, components of frequency less than the frequency of the fundamental voltage harmonic called subharmonics or subsynchronous interharmonics occur. In this paper, the effect of voltage subharmonics on currents, power losses, speed fluctuations and electromagnetic torque is examined. The results of numerical computations using the finite element method for an induction cage motor of rated power of 5.6 MW and four motors of rated power of 200 kW with different numbers of poles are presented. An extraordinary harmful effect on high-power induction motors is demonstrated. Among other effects, voltage subharmonics cause significant torque pulsations whose frequencies may correspond to the elastic-mode natural frequency. Possible resonance can result in excessive torsional vibration and the destruction of a power train.

Keywords: induction motors; interharmonics; power losses; power quality; power system; subharmonics; voltage fluctuations

1. Introduction

Voltage waveform distortions exert a noxious effect on various elements of a power system, which in extreme cases may pose a threat to human safety and the environment [1]. Distorted voltage waveforms generally contain harmonic components. However, in some cases, other undesirable components may occur, namely subharmonics (subsynchronous interharmonics) and interharmonics, which are components of a frequency that are less than the fundamental harmonics or are not its integer multiple, respectively.

One reason for a subharmonic appearance is the work of non-linear loads, such as inverters, cycloconverters and arc furnaces [2–7]. For instance, in [2], a high level of subharmonic contamination was reported in a building with a large number of computers and other non-linear loads situated in the nearby area of steel works. The maximal root of the sum of the squared subharmonic subgroups within the frequency range 5–40 Hz was 0.99% of the fundamental voltage harmonic (for 10-min aggregation time) and the mean value was 0.29%.

Subharmonic contamination also originates from the work of renewable sources of energy [3,8–10], such as wind power stations, photovoltaic plants and wave farms. The level of voltage subharmonics may be especially significant under abnormal working conditions, like the subharmonic resonance of a wind farm [10]. During an example resonance event, lasting 108 s, the voltage subharmonic of frequency 8.1 Hz reached 1–2% of the fundamental component (based on the additional information received from the authors of [10]). Subharmonics can also be injected into the power system by induction or by synchronous motors driving a load of pulsating torque [11,12]. It is also worth mentioning that periodic voltage fluctuation exerts the same effect on induction motors as the simultaneous presence of

voltage subharmonics and interharmonics [13] and can be regarded as a superposition of both power quality disturbances [3,13].

Subharmonic contamination may disturb the work of control systems, light sources, converters, power and measurement transformers, synchronous generators and induction motors [6]. In induction motors, it causes, among other effects, an increase in power losses and winding temperature, thermal loss of life, torque pulsation and vibration. It should be stressed that even apparently inconsiderable traces of voltage subharmonics may cause excessive vibration and heating of induction motors [14–16].

Although voltage subharmonics are an especially detrimental power quality disturbance, the related standards and power quality regulations do not impose a limitation on their values. In the standard EN 50160 Voltage characteristics of electricity supplied by public distribution systems [17], the following comment appears regarding voltage interharmonics (applying to subharmonics understood as a kind of interharmonic): "The level of interharmonics is increasing due to development of the application of frequency converters and similar control equipment. Levels are under consideration, pending more experience".

Initial recommendations concerning admissible levels of voltage subharmonics are proposed in [18,19]. The recommendations are motivated mostly by voltage subharmonics' extraordinarily detrimental impact on induction motors. The elaboration of final recommendations requires comprehensive investigations of various harmful phenomena caused by voltage subharmonics, including ones occurring in induction motors with various properties.

The effect of voltage subharmonics on induction machines was examined in [6,13–16,18–26]. It should be stressed that these works concern only low-power machines except [13,14,18,20] and the authors' preliminary work [25]. In [13,18], the investigations of high-power machines were restricted to thermal loss of life. The appropriate calculations were performed on the basis of a T-type equivalent circuit, which shows significant limitations for the analysis of induction motors under subharmonics [15,21]. Furthermore, in [13], fluctuations of the rotational speed and content of subharmonics and interharmonics in the supply current were analysed. The applied calculation method was based on dq transformation, which also shows significant limitations [26]. In [20], speed fluctuations, currents, torque pulsations and input and output power were analysed for a 100-kW under voltage fluctuation of one amplitude and frequency. Numerical calculations were carried out with the finite element method for various winding configurations.

To summarise, in the state of the art, there is a significant gap concerning the effect of voltage subharmonics on high-power induction motors. Above and beyond, in previous works, the problem of elastic-mode torsional resonance under subharmonics was not discussed. It is also worth mentioning that the effect of voltage subharmonics was not compared between machines of similar power and different numbers of poles.

The main purpose of this paper is to initiate research on possible elastic-mode resonance under voltage subharmonics. Additionally, the effect of subharmonics on speed fluctuations, currents, power losses and torque pulsations is analysed. The admissible subharmonic level, determined according to the criterion of machine heating, is discussed. The results of computations with the finite element method (FEM) are presented for a cage induction motor of rated power of 5.6 MW as well as for four motors of rated power of 200 kW and different numbers of poles. The scope of this study is limited to positive-sequence voltage subharmonics. The presented results of investigations should be useful for the elaboration of proposals of modifications of the power quality rules and standards.

2. Torque Pulsations and Resonance Phenomena

Voltage subharmonics cause flow through windings of both current subharmonics and interharmonics [13,16] of a frequency (based on [13]):

$$f_{ih} = 2f_1 - f_{sh} \tag{1}$$

where f_{ih}, f_{sh} and f_1 are the frequencies of current interharmonics, subharmonics and the fundamental voltage component, respectively.

Current subharmonics and interharmonics interact with the magnetic field excited by the fundamental voltage harmonic, and as a result, the electromagnetic torque contains a pulsating component of a frequency (based on [13]):

$$f_p = f_1 - f_{sh}. \tag{2}$$

$$f_p = f_{ih} - f_1 \tag{3}$$

Torque pulsations are interconnected with tangential electromagnetic forces, which are the major internal sources of vibration in induction machines under power quality disturbances [27]. Torque pulsations also cause fluctuations in the rotational speed. As a result, the application of the T-type equivalent circuit for the analysis of an induction machine under subharmonics may lead to large calculation errors [15,21].

To compound this problem, speed fluctuations cause a reaction of the electromagnetic torque analogous to the reaction of a torsional spring [11]. Consequently, for small moments of load inertia and torque pulsations of frequencies close to the natural frequency of the rigid-body mode ($f_{Nr\text{-}b}$), resonance phenomena may occur [15,16]. It should be noted that the frequency $f_{Nr\text{-}b}$ depends on machine power. For low-power machines, it is usually tens of hertz, and for large machines, it is of a few hertz [12]. Under rigid-body resonance, speed fluctuations boost current subharmonics and interharmonics, which additionally increase torque pulsations and speed fluctuations. The escalated speed fluctuations result in a further increase in current subharmonics and interharmonics. Consequently, for low-power machines and small moments of load inertia, current subharmonics and interharmonics can reach especially high levels [15,16]. Additionally, under rigid-body resonance, particularly high vibration can occur [16].

Under torque pulsations, elastic-mode resonance [28–32] may also appear, in which the elements of a power train act as a twisted torsional spring. The elastic-mode natural frequency can be determined with an experimental method [29], a dedicated software [31] or a mechanical dynamic lumped-parameter model [29–32]. In the model, a power train is represented by lumped masses connected with springs. It is worth adding that the mechanical model can be replaced with an equivalent electrical circuit [30] consisting of capacitances, inductances and resistances, representing damping [29,30]. As damping is usually low, it can be omitted (based on [29]) for a rough analysis.

The simplest model of rotating machinery is the one-mass system. The critical speed (ω_c) equals [31]

$$\omega_c = \sqrt{\frac{K}{m}} \tag{4}$$

where m is the mass [31] and K is the spring constant.

In practice, rotating machinery constitutes a multi-mass system. For such a system, the first critical speed (ω_{cmm}) can be approximated with Dunkerley's equation [31]:

$$\frac{1}{\omega_{cmm}^2} = \frac{1}{\omega_{c1}^2} + \frac{1}{\omega_{c2}^2} + \frac{1}{\omega_{c3}^2} \dots \tag{5}$$

where ω_{c1}, ω_{c2}, ω_{c3}... are the critical speeds of a system containing only mass one, mass two, mass three and so on.

Finally, for a two-inertia system and neglected damping, the natural frequency of the first elastic mode (f_{N1e}) can be assessed as [29]

$$f_{N1e} = \frac{1}{2\pi}\sqrt{K_t \frac{J_m + J_L}{J_m J_L}} \tag{6}$$

where K_t is the equivalent torsional stiffness, and J_m and J_L are the moments of motor and load inertia, respectively.

The first elastic-mode natural frequency is almost always below the grid frequency for large two-pole and four-pole motors driving turbomachinery [28]. For example, for a four-pole 6 100 kW motor driving a compressor, the natural frequency was 17 Hz [28]. Furthermore, for a six-pole 500 hp induction motor driving a fan, the natural frequency was reported as f_{N1e} = 24 Hz and f_{N1e} = 28.5 Hz depending on the coupling properties [29]. It should be stressed that elastic-mode torsional resonance causes a multiplication of torque pulsations. According to [29], torsional excitation may be amplified 50 times. As a result, excessive torsional vibration may lead to material fatigue and the crack of a shaft or a coupling [28,29].

In summary, for high-power induction motors, natural frequencies of both rigid-body and elastic-mode resonances may correspond to the frequency of torque pulsations due to subharmonics. Consequently, the resonance could significantly influence undesirable phenomena caused by the power quality disturbance under consideration.

3. Field Models

The research objects are low- and medium-voltage squirrel-cage induction motors produced by Zakład Maszyn Elektrycznych "EMIT" S.A. Cantoni Group (the second author's company; EMIT). Four of the motors are of power of 200 kW and, depending on the number of poles, are denoted as motor 2-p2, motor 2-p4, motor 2-p6 and motor 2-p8. The fifth investigated motor has a rated power of 5600 kW and is referred to as motor 56-p8 (see Figure 1 [33]). Their basic parameters are laid out in Table 1.

For the purpose of numerical analysis, the ANSYS Electronics Desktop environment (Ansys Electromagnetics Suite 18.0.0) was employed. The 2D models were generated from the RMxprt module on the basis of geometric dimensions and material properties. Winding resistances were assumed on the grounds of heating tests performed at EMIT. It should be noted that the authors had access to construction documentation and the test results of the motors due to the courtesy of the management board of EMIT. A standard Tau mesh (Figure 2), available in the Ansys Electromagnetics Suite 18.0.0, was used for the calculations. The applied meshes contain 4100 (motor 2-p8)–53,596 (motor 56-p8) triangular elements. Their maximal side dimensions are provided in Table 2. The integration step was assumed to be equal to 0.1 ms. It is also worth mentioning that total power losses occurring in a motor were assumed to be the sum of the following components calculated by Ansys Electromagnetics Suite: Core Loss, StrandedR and Solid Loss.



Figure 1. Photograph of motor 56-p8 (type Sfw 900 HV8D).

Table 1. Basic parameters of the investigated motors.

Motor	Motor 2-p2	Motor 2-p4	Motor 2-p6	Motor 2-p8	Motor 56-p8
Type	SLgm 315 ML2B	SEE 315 L4	3SIE 355 ML6A	SEE 355 ML8B	Sfw 900 HV8D
Rated power (kW)	200	200	200	200	5600
Number of poles	2	4	6	8	8
Rated rotational speed (rpm)	2982	1487	989	740	745
Rated frequency (Hz)	50	50	50	50	50
Rated voltage (V)	400 Δ	400 Δ	400 Δ	400 Δ	10500 Y
Rated current (A)	335	346	350	384	375
Rated efficiency (%)	95.8	95.9	95.8	95.2	96.8
Rated power factor (-)	0.90	0.87	0.86	0.79	0.85
Rated torque (Nm)	640	1284	1931	2581	71,785
Moment of inertia (kgm^2)	2.5	3.3	7.2	7.7	1581

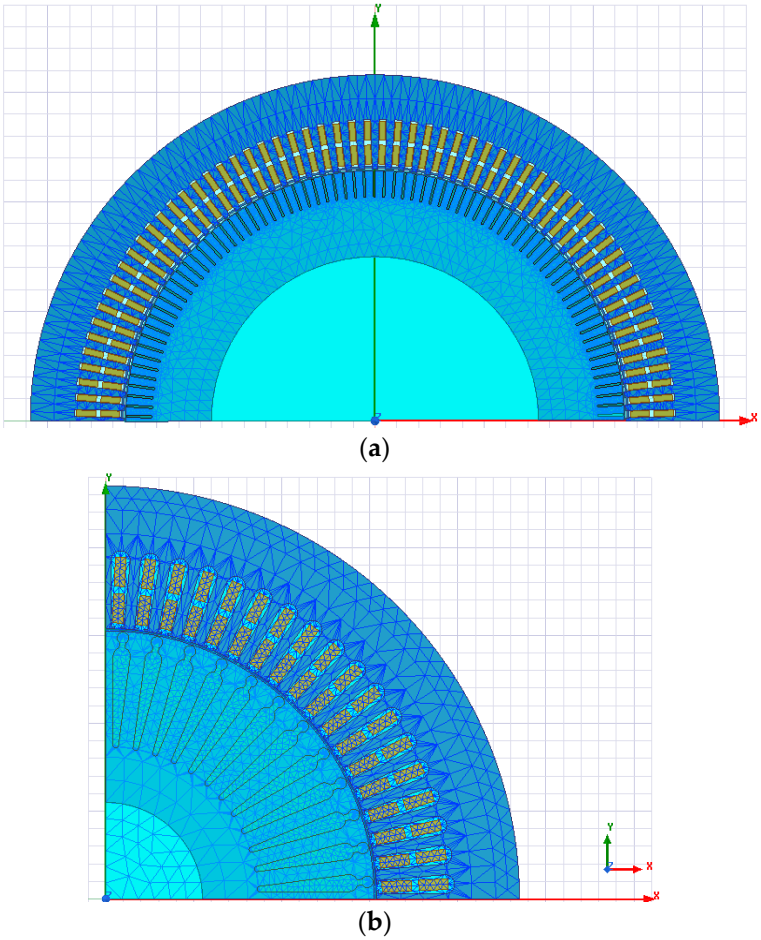


Figure 2. Mesh applied to (**a**) motor 56-p8 (type Sfw 900 HV8D) and (**b**) motor 2-p4 (type SEE 315 L4).

Table 2. Maximal side dimensions of finite elements.

Motor	Motor 2-p2	Motor 2-p4	Motor 2-p6	Motor 2-p8	Motor 56-p8
air gap (mm)	2.593	1.81	2.07	2.05	6.91
stator winding (mm)	7.27	4.33	4.44	4.21	8.73
rotor winding (mm)	6.36	4.84	4.35	3.7	2.5
other elements (mm)	22.36	16.43	16.16	16.14	57.34

The models were parameterised (calibrated) using the experimental data for the sinusoidal supply. Specifically, the rotational speed was pre-set as equal to its value determined during the heating tests of the motors. Then, the conductivity of the rotor cage material was adjusted to achieve equality

between the measured and calculated currents. It should be noted that this procedure was used by the second author in the design process of electrical machines. Furthermore, for calculations with variable rotational speeds, the load torque was adjusted to attain current convergence.

On account of the uncertainty of the parameters of the magnetic sheets (mostly), the calculated input power slightly differs from the measured one. The appropriate comparison is laid out in Table 3 for the 200 kW motors and the computations for variable rotational speeds. For motor 56-p8, the heating test was performed under substitute loading because of the high-rated power, and its model was calibrated using the rated data. It should be noted that due to the high power of the motors, experimental investigations under subharmonics injection would be very costly and difficult and for this reason were not carried out.

Table 3. Calculated and measured input power during heating test.

Motor	Motor 2-p2	Motor 2-p4	Motor 2-p6	Motor 2-p8
Measured input power (kW)	208.8	208.56	209.1	210.12
Calculated input power (kW)	213.3	214.56	212.35	216.66

Under subharmonic injection, phase voltages can be described with the following dependencies:

$$U_{phA} = U_{1m}sin(2\pi f_1 t) + U_{shm}sin(2\pi f_{sh} t) \tag{7}$$

$$U_{phB} = U_{1m}sin\left(2\pi f_1 t - \frac{2\pi}{3}\right) + U_{shm}sin\left(2\pi f_{sh} t - \frac{2\pi}{3}\right) \tag{8}$$

$$U_{phC} = U_{1m}sin\left(2\pi f_1 t - \frac{4\pi}{3}\right) + U_{shm}sin\left(2\pi f_{sh} t - \frac{4\pi}{3}\right) \tag{9}$$

where U_{phA}, U_{phB} and U_{phC} are phase voltages; U_{1m} and U_{sh} are magnitudes of the fundamental and subharmonic voltage components, respectively; and f_1 and f_{sh} are frequencies of the fundamental and subharmonic voltage components, respectively.

These phase voltages were set up using the Voltage of the Excitations parameter, available in the Ansys Electromagnetics Suite 18.0.0.

In the subsequent section, the induction motors under subharmonics are analysed using the presented field models.

4. Results

4.1. Considered Cases

In this section, the results of the research on speed fluctuations, currents, power losses and torque pulsations are shown. Admissible levels of subharmonics with respect to machine heating are also presented. All numerical computations are performed for voltage subharmonics equal to 1% of the fundamental voltage component, as similar levels are reported in [2,10]. As the moment of load inertia exerts a significant effect on undesirable phenomena in low-power machines under voltage subharmonics [15,16], two extreme cases are compared. The first concerns work with a load with a negligible moment of inertia (NMI), and the second concerns work with a constant rotational speed (CRS). In practice, this case corresponds to machines driving a load of moment of inertia much greater than the motors' moment. The numerical experiments were performed for the fundamental voltage component of the rated value. The load torque was assumed as equal to its rated value, independently of the rotational speed. It should be noted that for this torque–speed characteristic, the greatest impact of subharmonics on currents and power losses is expected [15]. The analysis time was 2 s, including a steady-state period lasting 1 s. The subharmonic content in the supply current was determined with fast Fourier transform.

4.2. Fluctuations of Rotational Speed

Fluctuations of the rotational speed are illustrated in Figure 3 and for NMI. For motor 2-p8, the amplitude is as high as about 1% of the rated rotational speed. For comparison, the rated slip is 1.33%. For the other investigated motors, the speed fluctuations present lower values, especially for motor 56p-8.

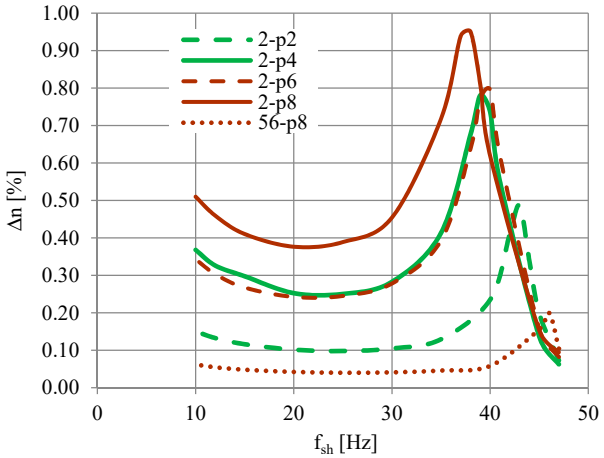


Figure 3. Amplitude of speed fluctuation (related to rated speed) vs. subharmonic frequency for motor 2-p2, motor 2-p4, motor 2-p6, motor 2-p8 and motor 56-p8; voltage containing subharmonics of value U_{sh} = 1% U_{rat}; and a negligible moment of load inertia.

The highest amplitude occurs for the subharmonics of frequency f_{sh} in the range 38 (motor 2-p8)–46 Hz (motor 56-p8). In this paper, the frequency corresponding to the maximum for each motor is denoted as f_{sh_max}. The peaks of the speed fluctuations (Table 4) are caused by rigid-body resonance (see Section 2). In practice, the frequency f_{sh_max} is approximately equal to (on the basis of [12,15])

$$f_{sh_max} \approx f_1 - f_{Nr-b} \tag{10}$$

Table 4. Amplitude of speed fluctuations (related to the rated speed) under rigid-body resonance.

Motor	Motor 2-p2	Motor 2-p4	Motor 2-p6	Motor 2-p8	Motor 56-p8
Amplitude of speed fluctuations (%)	0.486	0.781	0.795	0.951	0.200

The fluctuations of the rotational speed considerably affect currents, power losses and pulsations of electromagnetic torque.

4.3. Effect of Subharmonics on Current and Power Losses

Current subharmonics and interharmonics flowing through windings cause additional ohmic losses and machine heating as well as torque pulsations. Below, in Figures 4 and 5 and Table 5, the results of the investigations on currents and total power losses are presented. The results of the computations are related to the current and total power losses determined for the nominal supply (I_{nom} and ΔP_{nom}, respectively).

Current subharmonics (I_{sh}) are presented in Figure 4 against the frequency of voltage subharmonics (f_{sh}). For CRS and frequency f_{sh} = 10 Hz, the current subharmonics are up to I_{sh} = 33% for motor 2-p2. For frequency f_{sh} = 45 Hz, the current subharmonics do not exceed c. 6% of I_{rat} for all the motors under investigation. Furthermore, for *NMI* and f_{sh} = 10 Hz, the current subharmonics are of similar values to those for CRS. For the greater frequency f_{sh}, the current subharmonics first descend and then

reach a local maximum for the frequency close to f_{sh_max} (for the investigated motors the frequency is approximately equal to f_{sh_max}—1 Hz). For this frequency, the current subharmonics are as high as c. 14% of I_{rat} (motor 2-p2). It should be noted that for the frequency close to f_{sh_max}, the current waveform additionally contains an interharmonic (see Section 2) of comparable value to the current subharmonic. The differences between NMI and CRS result from speed fluctuations and rigid-body resonance around the frequency f_{sh_max} (the local maximum). Namely, the speed fluctuations amplify current subharmonics and interharmonics, which increase speed fluctuations even more. The shape of these characteristics significantly influences the dependency of power losses vs. subharmonic frequency, which is shown in the next diagram (Figure 5). For CRS and frequency f_{sh} = 10 Hz, the total power losses are between 108% of ΔP_{nom} (motor 2p-8) and 116% of ΔP_{nom} (motor 2p-4), while for the frequency f_{sh} > 30 Hz, the increase in power losses due to subharmonics is insignificant. Furthermore, for NMI, the power losses are as high as 118% of ΔP_{nom} (motor 2p-4, f_{sh} = 10 Hz). For the frequency f_{sh_max}, power losses do not exceed about 103% of ΔP_{nom}.

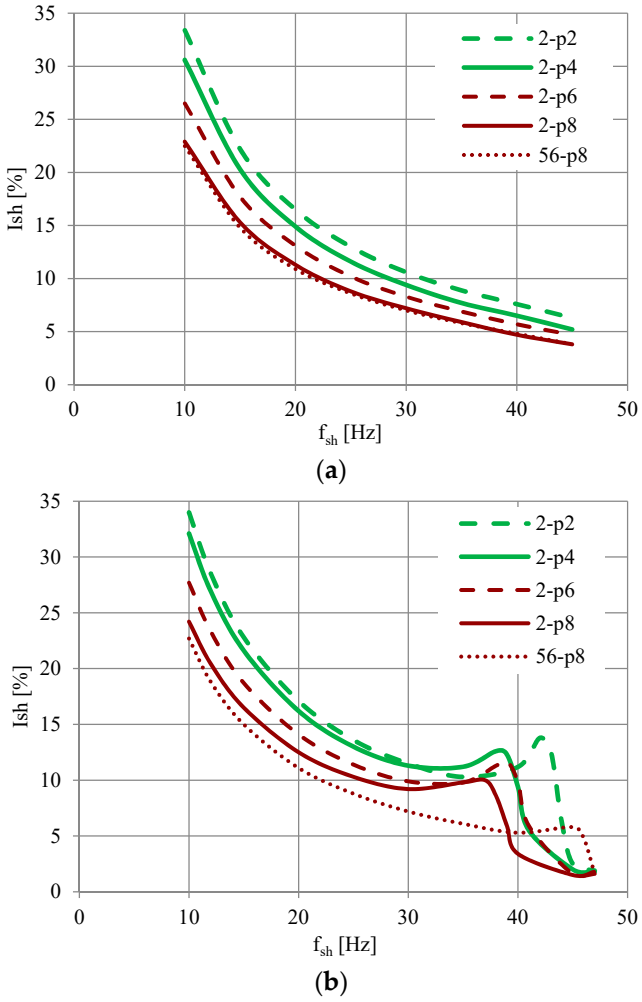
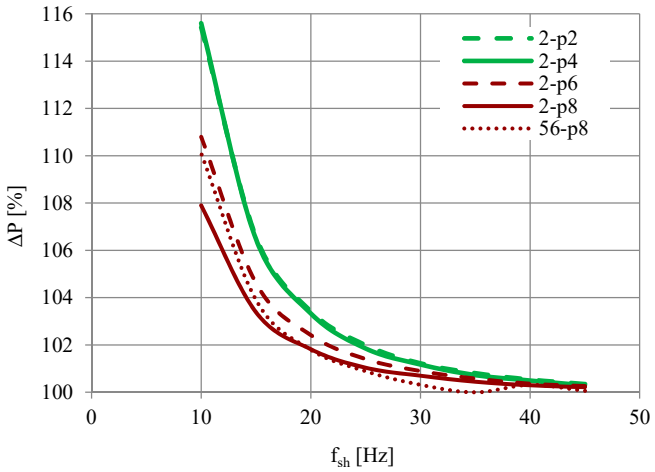


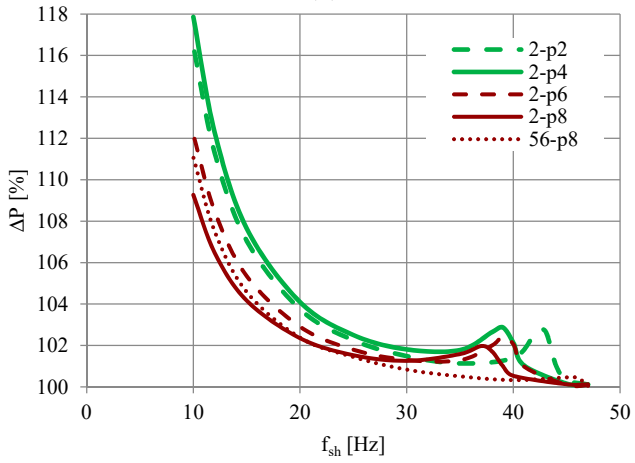
Figure 4. Current subharmonics vs. subharmonic frequency for motor 2-p2, motor 2-p4, motor 2-p6, motor 2-p8 and motor 56-p8; voltage containing subharmonics of value U_{sh} = 1% U_{rat}; (**a**) constant rotational speed due to the high moment of load inertia; (**b**) a negligible moment of load inertia.

Table 5. Current subharmonics and power losses (related to the rated current and total power losses), for a negligible moment of load inertia.

Motor	Motor 2-p2	Motor 2-p4	Motor 2-p6	Motor 2-p8	Motor 56-p8
Current subharmonics for f_{sh} = 10 Hz (%)	34.0	32.1	27.7	24.2	22.7
Current subharmonics under resonance (%)	13.8	12.6	11.7	10.0	5.8
Power losses for f_{sh} = 10 Hz (%)	116.4	117.9	112.2	109.3	111.1
Power losses under resonance (%)	102.7	102.9	102.4	102.0	100.5



(**a**)



(**b**)

Figure 5. Relative power losses (referring to its value under sinusoidal supply) vs. subharmonic frequency for motor 2-p2, motor 2-p4, motor 2-p6, motor 2-p8 and motor 56-p8; voltage containing subharmonics of value U_{sh} = 1% U_{rat}; (**a**) constant rotational speed due to the high moment of load inertia; (**b**) a negligible moment of load inertia.

It should be noted that the above characteristics significantly differ from analogous ones determined in [15] for an exemplary 3-kW induction motor. For low-power machines, moments of load inertia and possible rigid-body resonance exert a greater effect on current subharmonics and power losses.

In summary, the presence of low-frequency voltage subharmonics (e.g., 10 Hz) may result in current subharmonics of high value and a significant increase in power losses. The highest values of

current subharmonics and power losses occur for two- and four-pole motors, and the lowest values occur for motor 2-p8 and motor 56-p8. For high-power machines, the rigid-body resonance exerts a comparatively moderate effect on the current subharmonics and power losses.

4.4. Pulsations of Electromagnetic Torque and Resonance Frequencies

Even for a purely sinusoidal supply of voltage, the electromagnetic torque shows moderate pulsations due to the presence of teeth and slots. For the distorted voltage, the torque pulsations can be much greater. The impact of voltage subharmonics on torque pulsations is presented in Figure 6 and Table 6. For CRS, the amplitude of torque pulsations is up to c. 47% of T_{rat} for frequency f_{sh} = 10 Hz. For frequency f_{sh} > 20 Hz, it is below 28% of T_{rat} and declines with an increment in frequency. For NMI, the maximal value of torque pulsations is slightly greater than for CRS (up to 49% of T_{rat} for the frequency f_{sh} = 10 Hz). Additionally, the torque pulsations have a comparatively high value around the frequency f_{sh_max}, especially for motor 2p-8 (up to about 34% of T_{rat}). For other frequencies, the torque pulsations are especially significant for this motor. Consequently, it could be particularly exposed to vibration and torsional vibration due to subharmonics. Furthermore, for motor 56p-8, the torque pulsations do not exceed about 26% of T_{rat}. It should be noted that the differences between CRS and NMI can be explained with speed fluctuations and resonance phenomena (see the previous subsections). It is also worth mentioning that all the investigated 200-kW motors have rotor bars skewed by one slot pitch, but of different skew angles [34]. The smallest one is applied in the eight-pole motor 2p-8, for which the most significant torque pulsations occur. At the same time, according to the numerical experiments performed by the authors, an additional increase in the skew angle results in a reduction in the pulsating torque component caused by subharmonics. The in-depth explanation of this phenomenon will be the subject of future investigations.

The torque pulsations presented in Figure 6 and Table 6 are of extraordinary amplitude. To compound this problem, possible resonance could multiply the torsional excitation. Below, Table 7 presents the natural frequencies of the first elastic mode f_{N1e} for the investigated motors working with a load with a moment of inertia equal to 500% of the motor moment. The frequencies are estimated with (6) for exemplary flexible couplings [35]. Damping, the inertia of couplings and detailed load properties were not taken into account. Additionally, a shaft was assumed to be much more torsionally rigid than the couplings under consideration. The natural frequencies f_{N1e} specified in Table 4 are in the range of 14 (motor 56-p8)–32.5 Hz (motor 2-p4), corresponding to the frequency of torque pulsations due to subharmonics (that is in the range between 0 and the frequency of the fundamental voltage component—see Section 2). Furthermore, as mentioned in Section 2, for some power trains with large and medium induction motors, the natural frequency f_{N1e} is almost always less than the network frequency [28]. As a result, possible elastic-mode resonance might destroy a motor or a coupling. For this reason, voltage subharmonics should be considered to be more detrimental power quality disturbances than previous studies [6,13–16,18–26] have indicated. The problem of elastic-mode resonance under voltage subharmonics will be the subject of future investigations.

Table 6. Amplitude of torque pulsations (related to the rated torque) for a negligible moment of load inertia.

Motor	Motor 2-p2	Motor 2-p4	Motor 2-p6	Motor 2-p8	Motor 56-p8
Amplitude of torque pulsations for f_{sh} = 10 Hz (%)	48.7	43.4	42.5	46.0	25.9
Amplitude of torque pulsations under resonance (%)	30.3	27.8	29.7	33.6	9.8

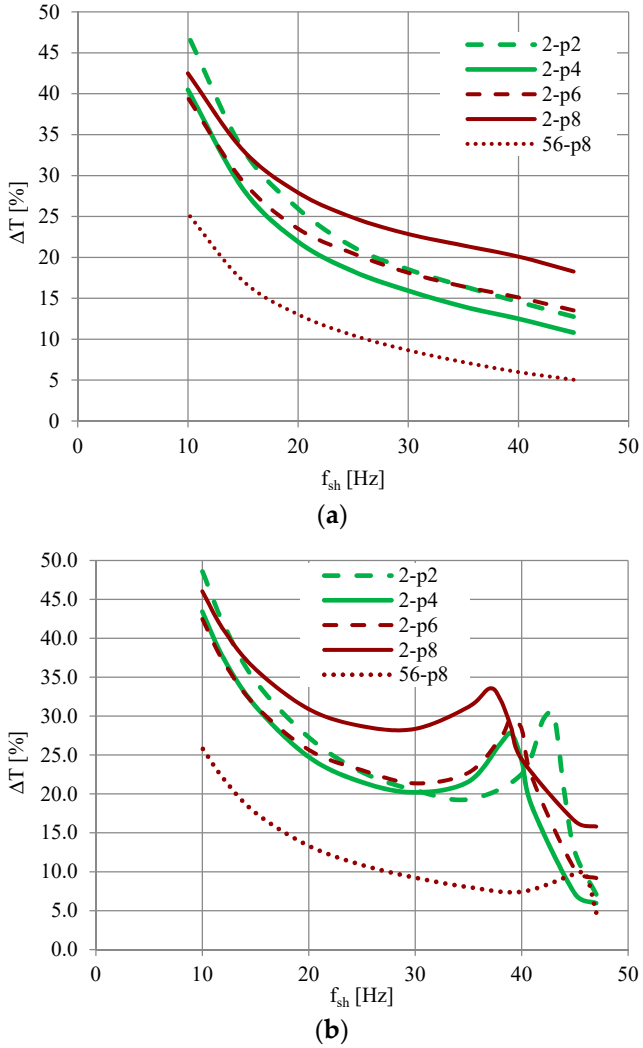


Figure 6. Amplitude of torque pulsations (related to rated torque) vs. subharmonic frequency for motor 2-p2, motor 2-p4, motor 2-p6, motor 2-p8 and motor 56-p8; voltage containing subharmonics of value U_{sh} = 1% U_{rat}; (**a**) constant rotational speed due to a high moment of load inertia; (**b**) a negligible moment of load inertia.

Table 7. Natural frequency of the first elastic mode (f_{N1e}) for exemplary flexible couplings and a moment of load of inertia equal to 500% of the motor moment.

Motor	Coupling	Dynamic Torsional Stiffness (kNm/Rad)	Natural Frequency (Hz)
Motor 2-p2	N-EUPEX B 200 1340 Nm	75	30
Motor 2-p4	N-EUPEX B 225 2000 Nm	115	32.5
Motor 2-p6	N-EUPEX B 280 3900 Nm	226	31
Motor 2-p8	N-EUPEX B 280 3900 Nm	226	30
Motor 56-p8	RUPEX RWN 800 110,000 Nm	10,700	14

5. Discussion

The previous proposals of subharmonic limitations [18,19] are partly based on the approximate analysis of machine heating. The simplest method to assess windings temperature rise is based on the calculation that it is proportional to the total power losses. At the same time, according to [15], voltage subharmonics of admissible levels should not cause an increase in windings temperature rise greater than 5%. Consequently, in this study, the admissible value of voltage subharmonics (U_{sh_p}) is

determined so that the total power losses are equal to 105% of ΔP_{nom}. The results of the numerical computations are presented in Figure 7 for NMI. It should be noted that the saddle in this chart corresponds to the peak in Figure 5b, discussed in Section 4.3. The least permissible subharmonic level occurs for motor 2-p4 and motor 2-p2. For frequency f_{sh} = 5 Hz, U_{sh_p} is merely 0.28% of U_{rat}. Furthermore, for frequency f_{sh} > 20 Hz, the value of U_{sh_p} exceeds 1% of U_{rat}, even under rigid-body resonance. For comparison, for an exemplary 3-kW induction motor, the value of U_{sh_p} determined for frequency f_{sh_max} = 20 Hz (rigid-body resonance) is 0.4% of U_{rat} [15]. Generally, high-power machines are less exposed to overheating due to subharmonics than low-power ones are, except for subharmonics of a frequency less than about 10–15 Hz. Contrastingly, voltage subharmonics might cause excessive torsional vibration, leading to the destruction of high-power induction motors.

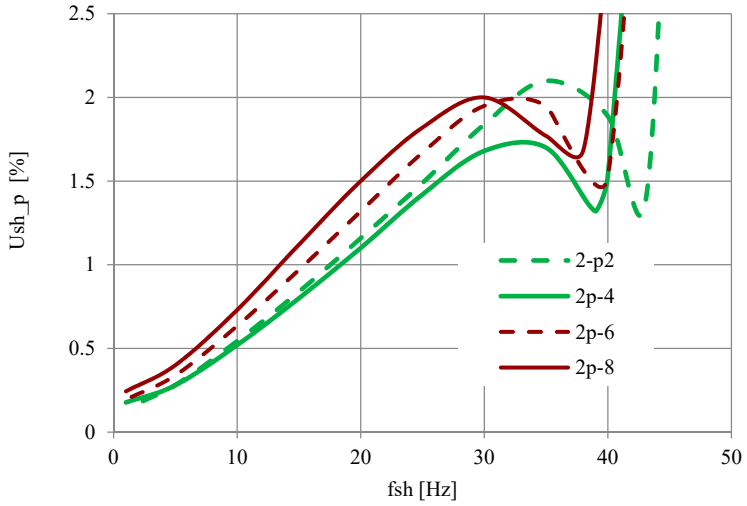


Figure 7. Permissible values of subharmonics U_{sh} (related to rated voltage) vs. subharmonic frequency for motor 2-p2, motor 2-p4, motor 2-p6 and motor 2-p8 and a negligible moment of load inertia.

On the basis of the above considerations, the results of the investigations presented in the previous subsections and [6,13–16,18–26], some indications concerning the determination of admissible levels for subharmonics are formulated. From the point of view of induction motors, the levels should be determined on the basis of the analysis of vibration and torsional vibration as well as the heating of high-power induction motors for a frequency f_{sh} less than about 10 Hz and the heating of low-power induction motors under rigid-body resonance.

Furthermore, in some power systems, extraordinary levels of voltage subharmonics were observed for a short period of time (see Section 1). At the same time, subharmonics are especially harmful in the case of long-lasting exposure, causing, for example, a thermal loss of motor life or fatigue of power train elements. For that reason, in the authors' opinion, the power quality standards and rules should specify two limit levels of subharmonics. The first of them should correspond to a long-term admissible value and could be based on 10-min aggregation time. The other one should concern the admissible instantaneous value. It worth mentioning that the proposed solution is based on provisions concerning voltage unbalance, included in the standard ICE 1000-2-4:1994 Electromagnetic Compatibility (EMC), Part 2–4: Environment—Compatibility Levels in Industrial Plants for Low-frequency Conducted Disturbances [36] (presently withdrawn). Determination of these limit levels requires additional investigation of a simultaneous effect of subharmonics of different frequencies and their harmful impact on various elements of a power system.

6. Conclusions

The effect of voltage subharmonics on an induction motor depends on various agents, including load and machine properties. The highest current subharmonics and increases in power losses are

observed in the two-pole and four-pole motors, and the highest torque pulsations occur in the eight-pole motor. Consequently, the machine could be especially exposed to harmful phenomena related to torque pulsations, like vibration and torsional vibration.

Torque pulsations are significantly affected by the frequency of subharmonics. The highest torque pulsations are reported for subharmonics of frequency $f_{sh} < 20$ Hz and under rigid-body resonance ($f_{sh} = 37$–46 Hz). For subharmonics of the value $U_{sh} = 1\%$ of U_{rat} and frequency $f_{sh} = 10$ Hz (which approximately corresponds to the voltage subharmonics reported in [10] for a short period of time), the amplitude of torque pulsations is as high as 49% of the rated torque. At the same time, for high-power machines, the frequency of torque pulsations may correspond to the natural frequency of the elastic mode. The possible occurrence of torsional resonance may significantly amplify torsional excitation and lead to the destruction of a motor or power train. For this reason, voltage subharmonics should be considered more harmful power quality disturbances than previous works have indicated and there is a need to carry out in-depth investigations on elastic-mode torsional resonance under subharmonics. Further, additional investigations are required to explain the effect of the constructional details of induction motors on undesirable phenomena under subharmonics, especially torque pulsations.

The presented results of the research also prove there is an urgent necessity to modify power quality rules and standards in order to protect energy receivers against the harmful effect of voltage subharmonics. In the authors' opinion, two limit levels of subharmonics should be introduced. The first of them should correspond a long-term admissible value and the other one to the admissible instantaneous value. Their determination requires further investigation of harmful phenomena caused by subharmonics.

Author Contributions: Conceptualisation, P.G.; methodology, P.K.; formal analysis, P.K.; investigation, P.K.; writing—original draft preparation, P.G. and P.K.; supervision, P.G. All authors have read and agreed to the published version of the manuscript.

Funding: This project is financially supported under the framework of a program of the Ministry of Science and Higher Education (Poland) as "Regional Excellence Initiative" in the years 2019–2022, project number 006/RID/2018/19, amount of funding 11 870 000 PLN.

Conflicts of Interest: The authors declare no conflict of interest. The funders had no role in the design of the study; in the collection, analyses, or interpretation of data; in the writing of the manuscript, or in the decision to publish the results.

References

1. Kumar, D.; Zare, F. Comprehensive review of maritime microgrids: System architectures, energy efficiency, power quality and regulations. *IEEE Access* **2019**, *7*, 67249–67277. [CrossRef]
2. Barros, J.; de Apraiz, M.; Diego, R.I. Measurement of subharmonics in power voltages. In Proceedings of the Power Tech 2007 IEEE Conference, Lausanne, Switzerland, 1–5 July 2007; pp. 1736–1740.
3. Bolen, M.H.J.; Gu, I.Y.H. Origin of power quality variations. In *Signal Processing of Power Quality Disturbances*; Wiley: New York, NY, USA, 2006; pp. 41–162.
4. Soltani, H.; Davari, P.; Zare, F.; Blaabjerg, F. Effects of modulation techniques on the input current interharmonics of adjustable speed drives. *IEEE Trans. Ind. Electron.* **2018**, *65*, 167–178. [CrossRef]
5. Soltani, H.; Davari, P.; Zare, F.; Loh, P.C.; Blaabjerg, F. Characterization of input current interharmonics in adjustable speed drives. *IEEE Trans. Power Electron.* **2017**, *32*, 8632–8643. [CrossRef]
6. Testa, A.; Langella, R. Power system subharmonics. In Proceedings of the IEEE Power Engineering Society General Meeting, San Francisco, CA, USA, 16 June 2005; Volume 3, pp. 2237–2242.
7. Yılmaz, I.; Ermis, M.; Cadırcı, I. Medium-frequency induction melting furnace as a load on the power system. *IEEE Trans. Ind. Appl.* **2012**, *48*, 1203–1214. [CrossRef]
8. Wen, Z.; Peng, S.; Yang, J.; Deng, J.; He, H.; Wang, T. Analysis of the propagation characteristic of subsynchronous oscillation in wind integrated power system. *Energies* **2019**, *12*, 1081. [CrossRef]
9. Xie, G.-L.; Zhang, B.-H.; Li, Y.; Mao, C.-X. Harmonic propagation and interaction evaluation between small-scale wind farms and nonlinear loads. *Energies* **2013**, *6*, 3297–3322. [CrossRef]

10. Xie, X.; Zhang, X.; Liu, H.; Liu, H.; Li, Y.; Zhang, C. Characteristic analysis of subsynchronous resonance in practical wind farms connected to series-compensated transmissions. *IEEE Trans. Energy Convers.* **2017**, *32*, 1117–1126. [CrossRef]
11. Arkkio, A.; Cederström, S.; Awan, H.A.A.; Saarakkala, S.E.; Holopainen, T.P. Additional losses of electrical machines under torsional vibration. *IEEE Trans. Energy Convers.* **2018**, *33*, 245–251. [CrossRef]
12. Arkkio, A.; Mölsä, E.; Holopainen, T.P. Reducing the losses of electrical machines under torsional vibration. In Proceedings of the 2018 XIII International Conference on Electrical Machines (ICEM), Alexandroupoli, Greece, 3–6 September 2018; pp. 1303–1309.
13. Tennakoon, S.; Perera, S.; Robinson, D. Flicker attenuation—Part I: Response of three-phase induction motors to regular voltage fluctuations. *IEEE Trans. Power Deliv.* **2008**, *23*, 1207–1214. [CrossRef]
14. de Abreu, J.P.G.; Emanuel, A.E. Induction motor thermal aging caused by voltage distortion and imbalance: Loss of useful life and its estimated costs. *IEEE Trans. Ind. Appl.* **2002**, *38*, 12–20. [CrossRef]
15. Gnaciński, P.; Pepliński, M.; Hallmann, D.; Jankowski, P. The effects of voltage subharmonics on cage induction machine. *Int. J. Electr. Power Energy Syst.* **2019**, *111*, 125–131. [CrossRef]
16. Gnaciński, P.; Pepliński, M.; Murawski, L.; Szeleziński, A. Vibration of induction machine supplied with voltage containing subharmonics and interharmonics. *IEEE Trans. Energy Convers.* **2019**, *34*, 1928–1937. [CrossRef]
17. Voltage Characteristics of Electricity Supplied by Public Distribution Network, EN Standard 50160, Brussels, Belgium, 2010.
18. de Abreu, J.P.G.; Emanuel, A.E. The need to limit subharmonics injection. In Proceedings of the 9th International Conference on Harmonics and Quality of Power, Orlando, FL, USA, 1–4 October 2000; Volume 1, pp. 251–253.
19. Fuchs, E.F.; Roesler, D.J.; Masoum, M.A.S. Are harmonics recommendations according to IEEE and IEC too restrictive? *IEEE Trans. Power Deliv.* **2004**, *19*, 1775–1786. [CrossRef]
20. Farah, M.J.; Abdollahi, R. An analytical investigation of induction motor behavior in the case of flicker occurrence using finite element method. *Univ. Politeh. Buchar. Sci. Bull. Ser. C Electr. Eng. Comput. Sci.* **2019**, *81*, 181–192.
21. Ghaseminezhad, M.; Doroudi, A.; Hosseinian, S.H.; Jalilian, A. Analysis of voltage fluctuation impact on induction motors by an innovative equivalent circuit considering the speed changes. *IET Gener. Transm. Distrib.* **2017**, *11*, 512–519. [CrossRef]
22. Ghaseminezhad, M.; Doroudi, A.; Hosseinian, S.H.; Jalilian, A. Analytical field study on induction motors under fluctuated voltages. *Iran. J. Electr. Electron. Eng.* **2020**, in press.
23. Ghaseminezhad, M.; Doroudi, A.; Hosseinian, S.H.; Jalilian, A. An investigation of induction motor saturation under voltage fluctuation conditions. *J. Magn.* **2017**, *22*, 306–314. [CrossRef]
24. Ghaseminezhad, M.; Doroudi, A.; Hosseinian, S.H.; Jalilian, A. Investigation of increased ohmic and core losses in induction motors under voltage fluctuation conditions. *Iran. J. Sci. Technol. Trans. Electr. Eng.* **2018**, *43*, 373–382. [CrossRef]
25. Gnaciński, P.; Klimczak, P. Preliminary study of a 200-kW induction motor supplied with voltages containing subharmonics. *Sci. J. Gdyn. Marit. Univ.* **2019**, *111/19*, 47–56.
26. Gnaciński, P.; Pepliński, M. Induction cage machine supplied with voltage containing subharmonics and interharmonics. *IET Electr. Power Appl.* **2014**, *8*, 287–295. [CrossRef]
27. Tsypkin, M. The origin of the electromagnetic vibration of induction motors operating in modern industry: Practical experience—Analysis and diagnostics. *IEEE Trans. Ind. Appl.* **2017**, *53*, 1669–1676. [CrossRef]
28. Bruha, M. Importance of control engineering to minimize torsional vibration in variable speed drive systems. In Proceedings of the 2016 Petroleum and Chemical Industry Conference Europe (PCIC Europe), Berlin, Germany, 14–16 June 2016; pp. 1–8.
29. Feese, T.; Ryan, M. Torsional vibration problem with motor/ID fan system due to PWM variable frequency drive. In Proceedings of the 37th Turbomachinery Symposium, Houston, TX, USA, 8–11 September 2008.
30. Kia, S.H.; Razavi-Far, R.; Saif, M. Torsional vibration identification using electrical signatures analysis in induction machine-based systems. In Proceedings of the 2018 IEEE 61st International Midwest Symposium on Circuits and Systems (MWSCAS), Windsor, Windsor, ON, Canada, 5–8 August 2018; pp. 813–816.
31. Oakes, B.K.; Donner, G.; Evon, S.T.; Paschall, T.W. A motor primer—Part 5. *IEEE Trans. Ind. Appl.* **2007**, *43*, 845–856. [CrossRef]

32. Yi, Y.; Tan, X.; Xuan, L.; Liu, C. Dynamic interaction behavior of an electric motor drive multistage gear set. *IEEE Access* **2020**, *8*, 66951–66960. [CrossRef]
33. Internal Documentation of Zakład Maszyn Elektrycznych "EMIT" S.A. Cantoni Group. Unpublished work, 2020.
34. Joksimović, G.; Melecio, J.I.; Tuoh, P.M.; Djurović, S. Towards the optimal 'slot combination' for steady-state torque ripple minimization: An eight-pole cage rotor induction motor case study. *Electr. Eng.* **2019**, *102*, 293–308. [CrossRef]
35. Flender. Configurators. Available online: https://www.flender.com/en/spice/overview (accessed on 20 May 2020).
36. *Electromagnetic Compatibility (EMC), Part 2–4: Environment—Compatibility Levels in Industrial Plants for Low-Frequency Conducted Disturbances*; IEC Standard 1000-2-4; IEC: Genova, Switzerland, 1994.

Publisher's Note: MDPI stays neutral with regard to jurisdictional claims in published maps and institutional affiliations.



© 2020 by the authors. Licensee MDPI, Basel, Switzerland. This article is an open access article distributed under the terms and conditions of the Creative Commons Attribution (CC BY) license (http://creativecommons.org/licenses/by/4.0/).